Article

Feasibility Study of Ground Source Heat Pump System Considering Underground Thermal Properties

Sang Mu Bae [1], Yujin Nam [2,*] and Byoung Ohan Shim [3] (ID)

[1] Department of Architectural Engineering, Pusan National University, 2 Busandaehak-ro 63, Geomjeong-gu, Busan 46241, Korea; trapezeb@naver.com
[2] Department of Architectural Engineering, Pusan National University, 2 Busandaehak-ro 63, Geomjeong-gu, Busan 46241, Korea; namyujin@pusan.ac.kr
[3] KIGAM, Gwahang-no 124, Yuseong-gu, Daejeon 305-350, Korea; boshim@kigam.re.kr
* Correspondence: namyujin@pusan.ac.kr; Tel.: +82-51-510-7652; Fax: +82-51-514-2230

check for updates

Abstract: A typical ground source heat pump (GSHP) system in South Korea has a ground heat exchanger (GHX) with a length of 100–150 m, which utilizes annually stable underground temperature to meet the loads of cooling, heating and hot water in buildings. However, most GSHP systems have been introduced in heating dominated areas because the system performance advantage is larger compared with air source heat pump system than that in cooling dominated areas. To effectively provide geothermal energy to the building in the limited urban area, it is necessary to install deep GHXs. Despite its large capacity, there are few studies on GSHP system with deep GHX over 300 m. In this study, to estimate the performance of the GSHP system with deep GHX and evaluate its feasibility, numerical simulation was conducted. To quantitatively analyze heat transfer between soil and GHX, the coupled model with GHX model and ground heat and groundwater transfer model was used. Furthermore, the heat exchange rate and the source temperature were calculated according to the operation modes, the length of GHX, and soil conditions such as geothermal gradient and thermal conductivity. As a result, the total heat exchange rate of GHX with a length of 300 m heat exchanger was 12.62 kW, 173% that of a length of 150 m. Finally, it was found that the GSHP system with deep GHX has realistic possibility in good condition of geothermal gradient.

Keywords: ground source heat pump (GSHP) system; ground heat exchanger (GHX); numerical simulation; geothermal gradient; heat exchange rate (HER)

1. Introduction

Recently, the efforts of the international society to respond to depletion of energy and climate change and realize sustainable development are continuing. Especially for the energy saving and energy independence in buildings, there have been many efforts using renewable energy technologies to meet increasing energy demands. Among the renewable energy technologies, the ground source heat pump (GSHP) system is very reasonable selection in building sector to meet the base load of heating, cooling and hot water without any weather condition effects. In addition, the GSHP system can achieve higher performance of system comparing with conventional air source heat pump (ASHP) system by utilizing more efficient underground temperature as heat source. Especially, this comparative advantage is more remarkable in the cold climate where air source heat pump system does not work well due to defrosting. Therefore, many studies on the GSHP system have been conducted in North America and northern Europe, and the market of GSHP has also been growing continuously. Especially,

Scandinavian countries and Finland utilize ground source heat pump (GSHP) system on a large scale. Since 2013, new houses in Finland had a GSHP introduced, and 8500 GSHP system units were sold in 2016 [1]. In addition, in North America, Cho et al. [2] evaluated the application feasibility for GSHP system of vertical type in residential and commercial buildings across seven climate zones in United States. As the result of residential buildings, the feasibility of GSHPs in cold climate zones was more than other climate conditions such as hot and mild climate zones.

Even though GSHP system has higher coefficient of performance (COP) than conventional ASHP system, the economic feasibility of GSHP system is not always assured in all projects. This system requires the installation of borehole and ground heat exchanger, and, in some cases, it is very expensive, according to geological and field conditions. Moreover, the performance of system also depends on the geological and hydraulic condition such as thermal conductivity, porosity, hydraulic conductivity and groundwater level [3,4].

Underground thermal potential including underground temperature is also significant factor. According to reports [5], the underground constant temperature zones are formed 1–6 m below the ground surface at the equatorial region and the tropical regions near the equator. In the case of the temperate regions, it is formed 10–15 m below the surface, and the temperature is similar to the annual temperature. Generally, the underground constant temperature zone could be located deeper if the place has lower moisture and dry soil, while it stays shallower if the soil contains higher moisture. As for the underground constant temperature zone, it is determined by the ground surface temperature, which is affected by the conduction, convection and radiation of the solar energy so that it differs in season and time of day. Therefore, the ground heat exchanger must be installed in deeper zone than common underground constant temperature zone to extract sufficient heat energy from the ground [6]. In addition, the underground temperature could gradually increase as the underground depth gets deeper. Regardless of the outside air temperature, it is influenced by heat extracted from the collapse of the radioactive elements consisting of the crust and released by the high temperature nucleus inside the earth. In the condition of high geothermal-gradient, the GSHP system with deep GHXs can be more effectively utilized than the conventional system.

There have been many studies about the variation of the underground temperature and system performance through numerical simulation and verification experiment on the purpose of distribution of the GSHP system using the deep ground heat exchanger. Holmberg et al. [7] studied the performance of the coaxial borehole heat exchanger at deep depth. A numerical model was developed to study the coaxial BHE and then the predicted performance of the model was compared with the results acquired from the TRT (thermal response test). Lous et al. [8] evaluated the influence from the design parameters of deep borehole heat exchanger (DBHE) and operation methods. The numerical model was devised to analyze the mass and heat flow of constant porous soil about 5 km vertical near the DBHE. This research established a foundation of a feasible and sustainable thermal use of DBHE. Michopoulos and Kyriakis [9] indicated that the system performance is affected by the fluid outlet temperature of the vertical ground heat exchangers. In addition, a numerical model predicting the fluid temperature was suggested considering the underground heat transfer and the time difference of the thermal load of the ground heat exchanger. Chen et al. [10] estimated the vertical GHE model with nine different parameters including thermal conductivity, inlet water temperature (IWT), groundwater flow, borehole depth and underground soil characteristics, to develop the optimum design. Li et al. [11] developed a program for the ground heat exchanger to analyze the heat transfer performance of the ground source heat pump system utilizing dynamic indoor load and actual operation characteristics as input data. Park and Park [12] calculated the variations of ground heat exchanger lengths depending on various design parameters such as thermal resistance of borehole, initial underground temperature, U-tube diameter and arranging method using GLD simulation. Kim [13] analyzed the influence of g-function (geothermal response function) obtained from different boundary conditions on the design of ground heat exchanger. As the result of using the FLS-N boundary condition, it was indicated that the length of the ground heat exchanger becomes longer than that under the Eskilson condition. Shin et al. [14]

figured out the geothermal boundary conditions and hourly underground temperature to utilize geothermal energy. The underground temperature was measured about 2 m below the surface in Tongyeong, South Korea and compared with results from the numerical analysis and then the accuracy was verified. As a result, the temperature difference highly influenced the outdoor temperature at 1 m below the ground surface, but it decreased deeper in ground. Min and Choi [15] studied the design length of the ground heat exchanger considering various design parameters such as underground thermal conductivity, GHE pipe diameter, and spacing. This study shows that the rise of the grout thermal conductivity made the greatest decrease of the length of the GHE. Ryoo et al. [16] analyzed the temperature and the calorific value of the circulating water which changes the flow rate inside the GHE, to effectively extract the geothermal energy with the vertical closed-type GHE using the deep geothermal energy. However, there are few studies on performance analysis of GSHP system with deep GHXs considering with heat exchange rate according to underground thermal properties and the design method of geothermal system using deep well has not been established.

In general, the geothermal gradient differs in location because of the different geothermal heat fluxes flowing from the underground to the ground surface and the thermal conductivity of the soil and rock. In the case of Japan, the geothermal gradient is estimated as 18–28 °C/km in southwest Gifu Prefecture and it is 100 °C/km in the active geothermal area southwest of the Ishikari plain of Hokkaido [17]. In addition, geothermal gradient predicted 23 °C/km and 24–28 °C/km in New York and the western of Pennsylvania, United States [18]. In the case of South Korea, it was identified that the average geothermal gradient is about 20–25 °C/km, and the geothermal anomaly areas having high heat flux, Bugok and Yesan, have about 76–83 °C/km gradient [5,19]. Even though the installation cost of GHX is a barrier against wide spread of GSHP system, in these local conditions, the deep GHX could be economical method for energy saving.

In this study, to determine suitable condition for GSHP system using deep GHX and effectively use it in urban area, the estimation of the system performance was conducted for various geological conditions and operation conditions. Moreover, a coupled simulation with the groundwater and ground heat transfer model, the ground heat exchanger model and the surface heat flux model was conducted to accurately analyze the system performance according to the installation condition and operation method. In the simulation, the heat exchange rate and COP (coefficient of performance) were calculated and the installation condition such as the depth of the ground heat exchanger, underground thermal properties and operation method of the GSHP system were considered.

2. Research Method

2.1. Deep Ground Heat Exchanger

Generally, the GSHP systems with vertical-closed type are installed at the depth of 100–200 m. It is because many installers think that the cost performance is the highest in the average underground condition. The performance and feasibility of the GSHP system depend on the underground condition such as thermal conductivity, rock composition, geothermal gradient, etc. Accordingly, the GSHP system using the deep ground heat exchanger of more than 300 m can be more efficient with high enough temperature heat source than the ordinary system. In this study, a deep GHX was assumed with a length of >300 m (Figure 1). Furthermore, the performance of deep GHX was quantitatively analyzed by heat source temperature and heat exchange rate through the coupled simulation with a groundwater and heat transfer model, a ground heat exchanger model and a surface heat balance model.
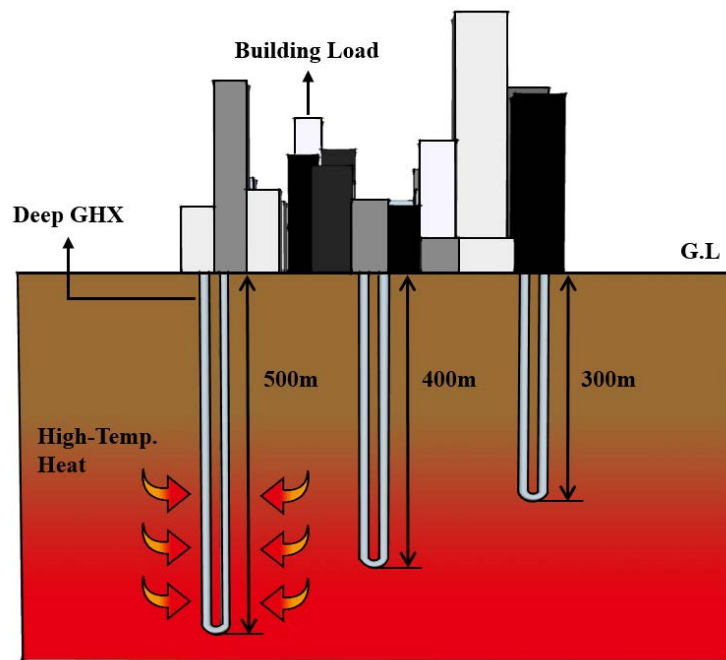
Figure 1. Concept of the deep ground heat exchanger.

2.2. Overview of the Simulation

To accurately analyze the heat transfer between the ground heat exchanger and the soil, a groundwater and heat transfer model (FEFLOW) was used. This simulation code is based on the finite element method and is widely used in the fields of groundwater movement and pollution. It can be used to analyze the transfer of geothermal and groundwater within the soil [20]. The simulation model was built by three-dimensional modeling that satisfies three laws, namely conservation of mass (Equation (1)), conservation of momentum (Equation ((2)), and conservation of energy (Equation ((3)), which classify the ground with three phases of solid, liquid and gas [21].

Law of conservation of mass:

$$\frac{\partial}{\partial t}(\epsilon_\alpha \rho^\alpha) + \frac{\partial}{\partial x_i}(\epsilon_\alpha \rho^\alpha v_i^\alpha) = \epsilon_\alpha \rho^\alpha Q_\rho^\alpha \tag{1}$$

Law of conservation of momentum:

$$v_i^\alpha + \frac{k_{ij}^\alpha}{\epsilon_\alpha \mu^\alpha}\left(\frac{\partial \rho^\alpha}{\partial x_i} - \rho^\alpha g_i\right) = 0 \tag{2}$$

Law of conservation of energy:

$$\frac{\partial}{\partial t}(\epsilon_\alpha \rho^\alpha E^\alpha) + \frac{\partial}{\partial x_i}(\epsilon_\alpha \rho^\alpha v_i^\alpha E^\alpha) + \frac{\partial}{\partial x_i}(J_{iT}^\alpha) = \epsilon_\alpha \rho^\alpha Q_T^\alpha \tag{3}$$

Heat Flux is described as follows:

$$J_{iT}^\alpha = -\left(\lambda_{ij}^{cond} + \lambda_{ij}^{disp}\right)\frac{\partial T}{\partial x_i} = -\epsilon_\alpha[(\lambda^\alpha + c^\alpha \rho^\alpha \alpha_t v^\alpha)\delta_{ij} + c^\alpha \rho^\alpha(\alpha_l - \alpha_t)\frac{v_i^\alpha v_j^\alpha}{v^\alpha}]\frac{\partial T}{\partial x_i} \tag{4}$$

Equation (5) presents the calculation model of a ground heat exchanger. It is based on the one-dimensional advection diffusion equation to calculate the temperature of the pipe surface and the circulation water at each depth point.

One-dimensional advection diffusion equation:

$$\frac{\partial T_w}{\partial t} = -\frac{\lambda_w}{\rho_w c_w} \times \frac{\partial^2 T_w}{\partial z^2} - U_w \frac{\partial T_w}{\partial z} + \frac{hP_w}{\rho_w c_w A}(T_1 - T_w) \tag{5}$$

In the one-dimensional advection diffusion equation, convective heat transfer can be expressed as Equation (6), and Equation (7) presents Nusselt number in circulating water turbulent flow inside the GHX that Dittus–Boelter devised.

Convective heat transfer:

$$h = Nu\frac{\lambda_w}{r} \tag{6}$$

Nusselt number:

$$Nu = 0.023Re^{0.8}Pr^n \tag{7}$$

here, n is 0.3 and 0.4 for cooling and heating, respectively. The ground surface heat balance model consists of solar radiation, sky radiation, ground surface radiation, convection and evaporation. The validity of the coupled simulation method was verified by comparative analysis with the verification experiments in the previous research [22].

Figure 2 shows the outline of analysis method in this study. The system used in this study consists of the GSHP system coping with the cooling and heating load of the building and the deep ground heat exchanger being able to extract a high-temperature heat source. The deep ground heat exchanger was set as one vertical-closed type with 300 m, 400 m and 500 m depth, respectively. The simulation was conducted using a numerical analysis model to accurately predict the ground heat exchange rate.
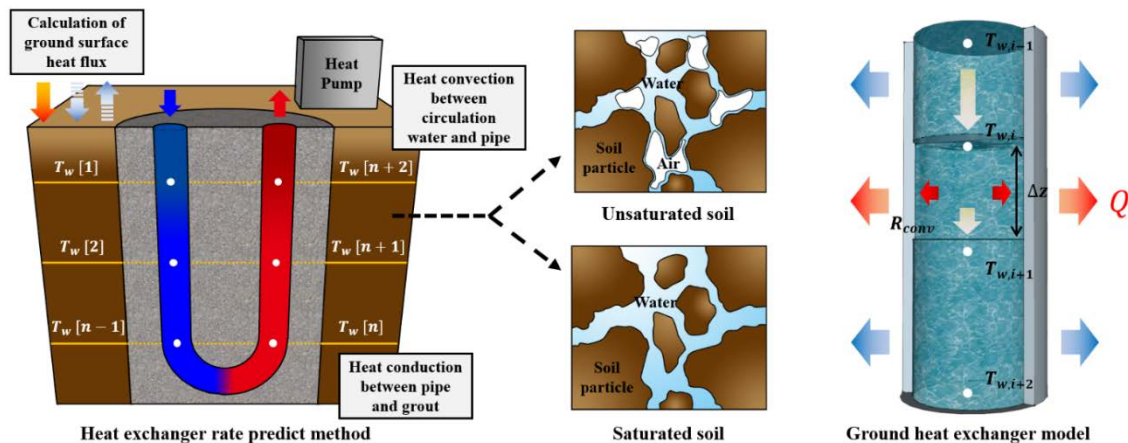
Figure 2. Outline of analysis method.

Figure 3 shows an analysis model to predict underground heat exchange rate of the GSHP system using the deep ground heat exchanger used in this study. To make sure the accuracy of predicting the heat extraction rate of the system, "Tetra-mesh" was utilized in the model to construct soil, grout and U-tube form. With analysis range of 20 m × 20 m, three analysis models were constructed depending on the borehole depth, at 300 m, 400 m, and 500 m. The borehole of 0.15 m diameter was installed at the center of the analysis area, grouted with concrete, and inserted with the ground heat exchanger (Single U-tube 50 A, Inner diameter: 0.0454 m, Outer diameter: 0.05 m). The spacing between the U-tubes was set as 0.075 m in consideration of the thermal interference between the ground heat exchangers. It was assumed that the ground condition was granite, which is the bed rock in South Korea, and the conditions for thermal property values of soil, grout and ground heat exchanger are shown in Table 1.
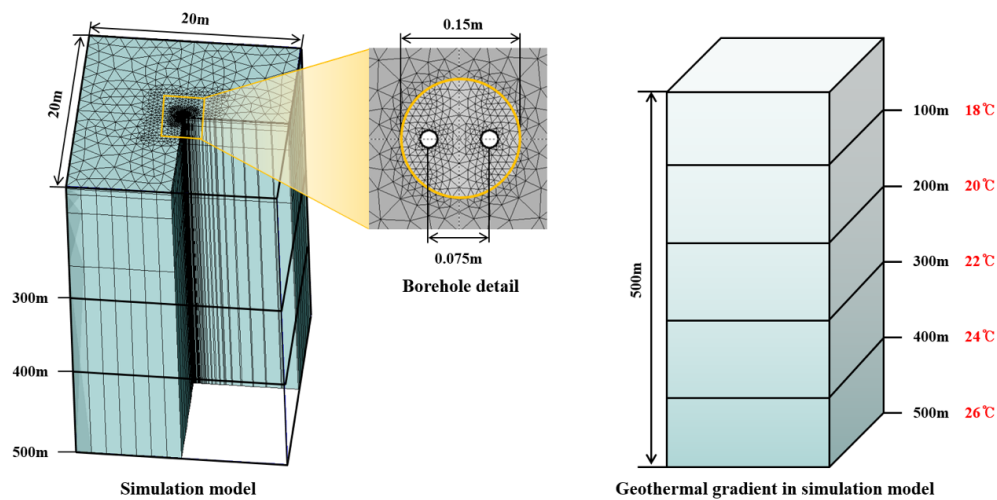
Figure 3. Simulation model.

Table 1. Ground, borehole and U-tube properties.

	Porosity	**Thermal Conductivity (W/m·K)**	**Thermal Capacity (MJ/m³·K)**
Granite	0.01	3.53	2.92
Concrete	0.001	1.5	2.8
U-tube	0.001	0.41	2.38

It was assumed that the system operation time is 9 h from 9:00 to 18:00, and the operation period is three months of winter for heating from 1 December to 28 February. The geothermal gradient can be described as the rate of the temperature difference according to the depth of the ground.

Geothermal gradient:

$$G = \frac{\partial T}{\partial z} \tag{8}$$

However, in this study, the initial underground temperature was set as 16 °C, and it increased 0.02 °C per meter based on the average geothermal gradient of South Korea. The three-dimensional numerical analysis model divided each layer with the depth of the ground heat exchanger, and the geothermal gradient values were applied on it. Table 2 represents the case study conditions.

Table 2. Case study conditions.

Case	GHX Length (m)	Thermal Conductivity (W/m·k)	Geothermal Gradient (°C/m)	Flow Rate (m/s)	Limit Temperature (°C)
1	150	3.5			
2		3.5			
3	300	3.0			
4		2.5			
5		3.5	0.02		
6	400	3.0		0.292	
7		2.5			
8		3.5			5
9	500	3.0			
10		2.5			
11	500		0.05		
12	500		0.1		
13	300				
14	400	3.5		0.3504	
15	500		0.02		
16	300				
17	400			0.292	0
18	500				

The case study of the GSHP system using the deep ground heat exchanger was conducted on the following design factors: ground heat exchanger depth, thermal conductivity, geothermal gradient, flow rate, system and limit temperature to accurately estimate the performance of the heat exchange rate. The numerical simulation model was set as 500 m, 400 m, and 300 m, respectively, to compare the effect of the depth of the ground heat exchanger on the performance of the heat extraction, and this study quantitatively analyzed the amount of heat exchange rate with different design factors.

Case 1, which describes a commonly-spread vertical type geothermal system, was used to evaluate and compare the performance of a geothermal system using a deep groundwater heat exchanger.

In general, the ground thermal conductivity has the greatest influence on the vertical closed GSHP system, and it also works as a key design factor to improve the performance of the deep ground heat exchanger. In Case 2, the ground thermal conductivities of three cases were set as 3.5 W/m·K, 3.0 W/m·K and 2.5 W/m·K, respectively, which is applied to Case 10, to analyze the heat extraction performance of the GSHP system according to the ground thermal conductivity. Cases 11 and 12 were utilized to analyze the possibility of the introduction and the underground heat extraction of the system according to the geothermal gradient, when a deep ground heat exchanger is installed in a region where the temperature slope of the geothermal gradient is high. The heat exchange rate of the GSHP system is defined by Equation (9).

Heat exchange rate:

$$Q = \frac{C\rho v A \Delta T}{d} \tag{9}$$

In Equation (9), it is possible to recognize that the heat exchange rate of the GSHP system is proportional to the heat source water flow rate. This way, an increase in the flow rate of the heat source water represents the heat exchange rate of the GSHP system to increase. In Cases 13–15, the flow rate of the heat source water was set to 0.3504 m/s in each depth of the ground heat exchanger, to analyze its influence on the performance of the heat extraction. Besides, the heat source water was set to prevent the decrease of underground temperature during the system operation. In general, the limit temperature of the heat source water is set to 5 °C; however, this study sets the heat source water temperature to 0° in Cases 16–18 considering the use of deep heat exchanger supplying a high temperature heat source.

3. Simulation Results

3.1. Comparison of the Heat Exchange Rate Length of the GHX

Figure 4 shows the inlet and outlet temperature of the heat source water and the HER during the operation period of Base Case (Case 1). Looking at the temperature of the heat source water for seven days after the start of the system operation, the gap between inlet and outlet temperature of the heat source water is gradually decreasing compared to the previous day since the ground temperature has not been fully recovered. Likewise, the amount of HER gradually decreases during the operation period as time passes. Therefore, this paper evaluated the performance of each case by averaging the total HER and the outlet temperature of the heat source water for three months.
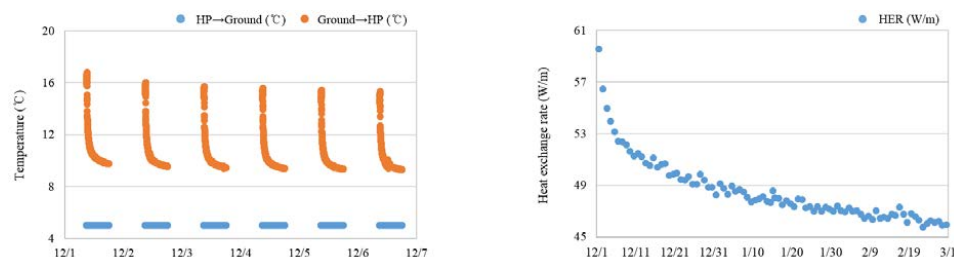

Figure 4. EWT (Entering Water Temperature) and HER (Heat Exchange Rate) of base case.

Figure 5 indicates the HER of geothermal system with an unusual 300 m long deep GHX and a general 150 m long GHX. The HER per unit meter was determined to be as 48.58 W/m in Case 1 (*d*: 150 m), which is 6.5 W/m higher than that of Case 2 (*GHX*: 300 m). However, regarding the total HER per unit borehole, Case 2 (*GHX*: 300 m) had approximately 73% higher amount than that of Case 1 (*GHX*: 150 m), and there was 5.34 kW difference in HER. In this respect, since the longer the length of the GHX, the higher the heat source temperature, due to the geothermal gradient, it is considered that a higher temperature of the heat source was supplied to the deep GHX, which made the total HER per unit borehole increased.
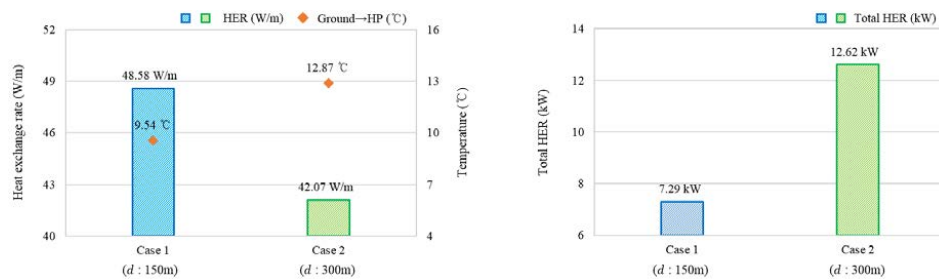
Figure 5. Comparison of the HER in different length of the GHX: Case 1 (GHX: 150 m); and Case 2 (GHX: 300 m).

Figure 6 indicates the distribution of underground temperature for Cases 1 and 2. The underground heat source temperature was measured at 5:00 p.m., the start of system operation (1 December) and the end of system operation (28 February). The underground heat source temperature of Case 2 was higher than Case 1 at the end of system operation. The underground heat source temperature difference was confirmed as 3 °C, and Case 2 actively utilized the underground heat source more than Case 1.
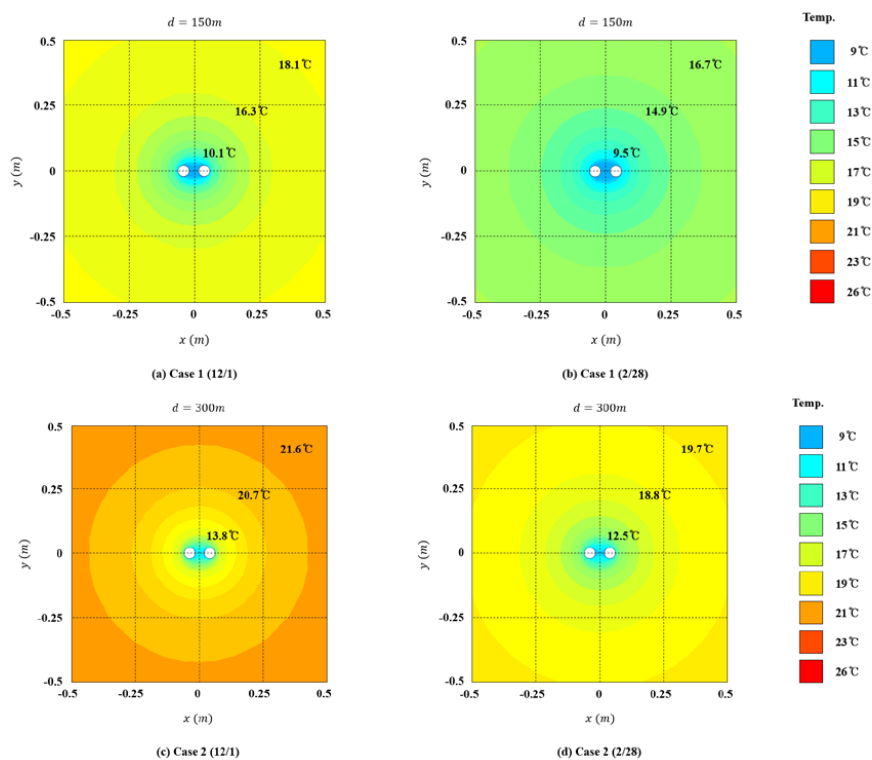
Figure 6. Distribution of underground temperature: Case 1 (*GHX*: 150 m); and Case 2 (*GHX*: 300 m).

3.2. EWT and HER According to Legnth of GHX

Figure 7 indicates the HER and the outlet temperature of the heat source water according to the underground thermal conductivity and the length of the GHX. Case 1 (λ: 3.5 W/m·K, *GHX*: 150 m) had the highest HER; the HER of Case 1 was increased by 40% at the maximum compared to that of Case 8 (λ: 3.5 W/m·K, *GHX*: 500 m), and its difference was determined to be as 13.97 W/m. However, the outlet temperature of the heat source water was 6.25 °C higher in Case 8 (λ: 3.5 W/m·K, *GHX*: 500 m) compared to that of Case 1 (λ: 3.5 W/m·K, *GHX*: 150 m). Thus, it was confirmed that the longer the length of the GHX, the lower the amount of the HER, but the potential to utilize a higher temperature heat source is improved.
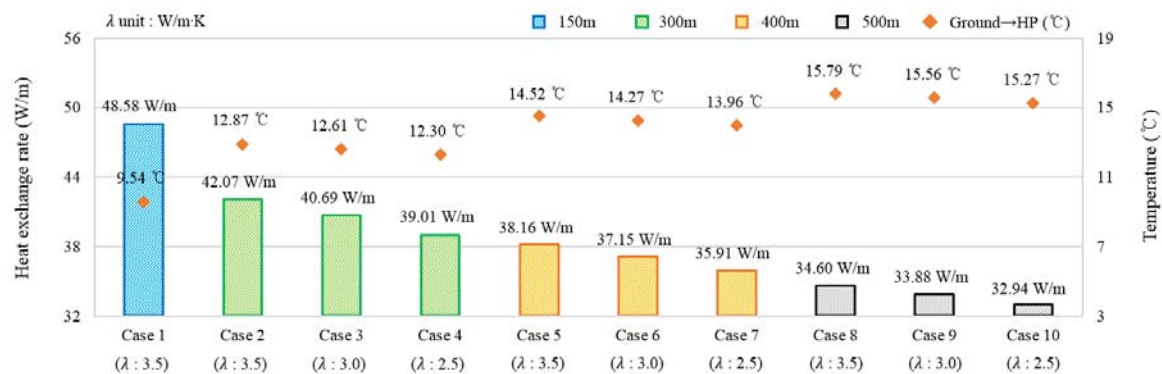
Figure 7. EWT and HER according to the thermal conductivity and the length of the GHX.

Figure 8 describes the total HER per one borehole and the outlet temperature of the heat source water according to the underground thermal conductivity and the length of the GHX. Under the same length of the GHX, the HER per one borehole was increased as the ground thermal conductivity raises. It was figured out that the difference of the HER according to the underground thermal conductivity was determined to be as 0.92 kW, which was the largest at 300 m length of the GHX.
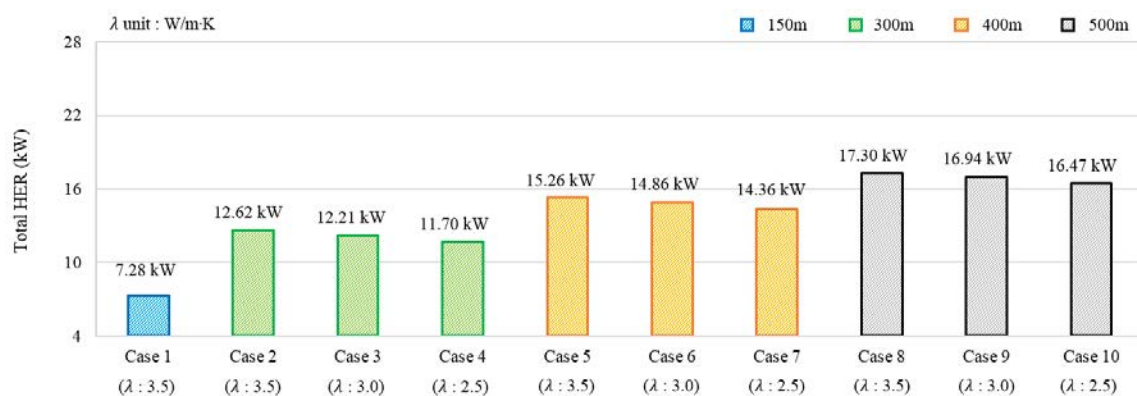
Figure 8. Total HER per borehole according to the thermal conductivity and the length of the GHX.

As shown in Figure 6, the HER per unit meter seemed to decrease as the length of the GHX increases, although the HER per borehole increased with the length of the GHX. Especially, the HER per borehole in Case 8 (λ: 3.5 W/m·K, *GHX*: 500 m) was the highest as 17.30 kW among Cases 1–10. Comparing the HER of Case 8 and Case 1 (λ: 3.5 W/m·K, *GHX*: 150 m), it was confirmed that the performance was 1.4 times different and the temperature of the heat source water showed a difference of 6.24 °C. In this respect, it is confirmed that the longer is the length of the GHX, the greater is the HER per borehole by using a higher heat source temperature in the ground.

Figure 9 shows the HER according to the geothermal gradient under the condition of 500 m length of the GHX. A case study was conducted to estimate the HER of deep GHX according to the geothermal gradient when it is installed in the region where the slope is high. The HER of Case 12 (*G*: 0.1 °C/m) was 29.19 W/m higher than that of Case 8 (*G*: 0.02 °C/m), which was increased up to 84%. In addition, the difference of the outlet temperature of the heat source water according to the geothermal gradient was 12.85 °C at the maximum. As a result, the higher the geothermal gradient, the greater the amount of the HER of the system.
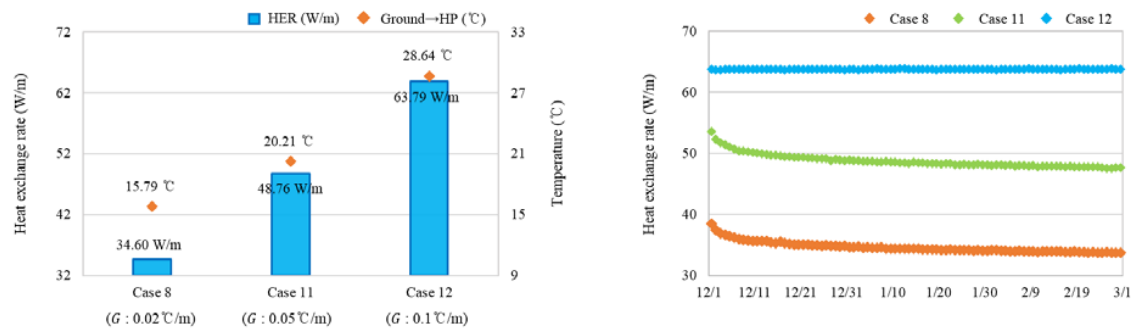
Figure 9. EWT and HER according to the geothermal gradient.

On the other hand, the slope of the HER becomes constant during the system operation, as the geothermal gradient increases. The higher geothermal gradient further enhanced not only the HER but also the potential to extract the geothermal heat. Therefore, it is considered that the system performance can be improved through the operation method which maximizes the potential of the system by installing the deep GHX in the region where the geothermal gradient is excellent.

Figure 10 indicates the distribution of underground temperature for Cases 8, 11 and 12. The underground heat source temperature was measured at 5:00 p.m., the start of system operation (1 December) and the end of system operation (28 February). The temperature of the underground heat source decreased significantly as the geothermal gradient increased, and the temperature difference was 28.2 °C maximum at the initial temperature. The higher is the temperature gradient, the lower is the temperature of underground heat source. However, the heat source temperature was confirmed to be high even at the end of operation. It is necessary to develop a method that can utilize heat source positively.
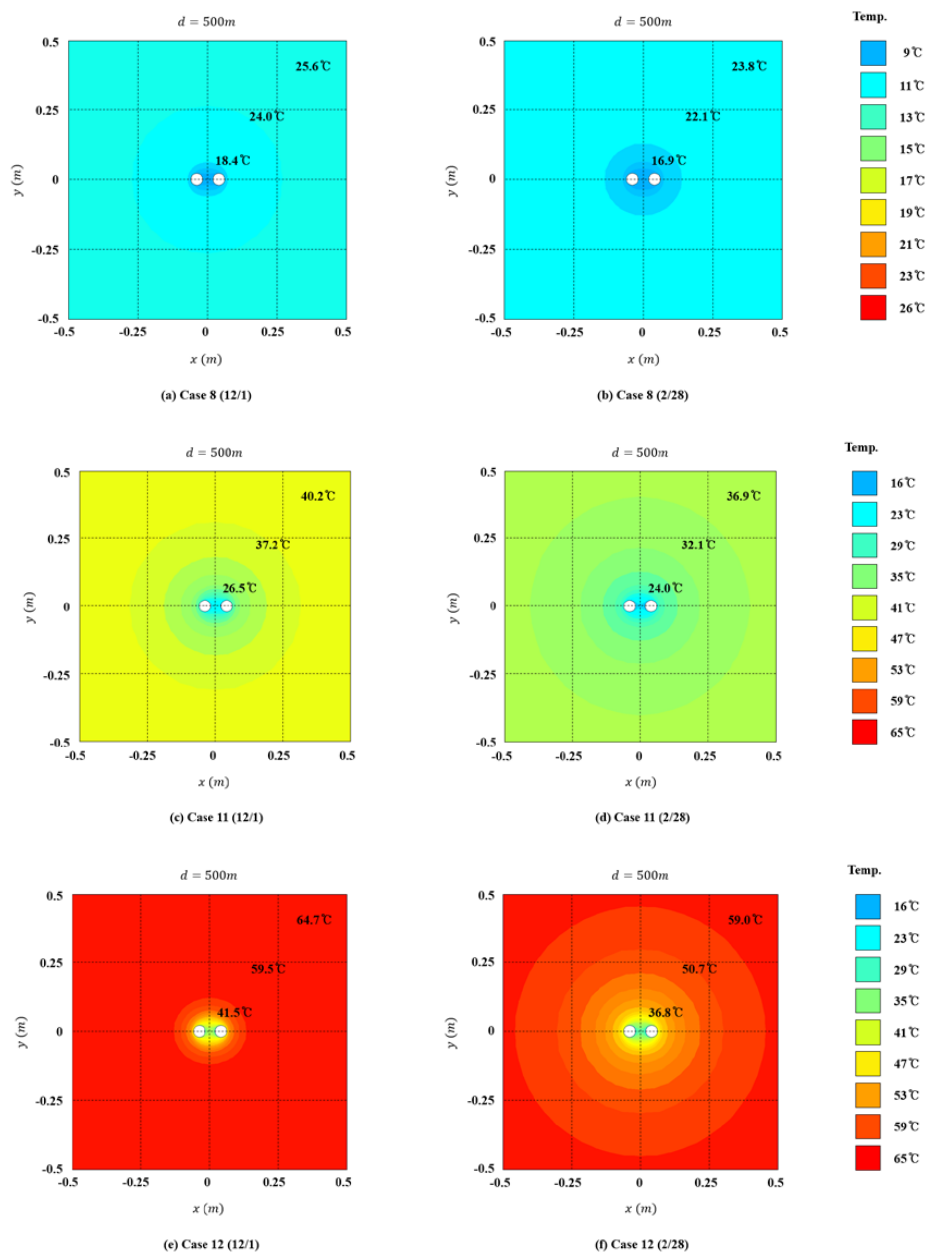
Figure 10. Distribution of underground temperature: Case 8 (G: 0.02 °C/m); Case 11 (G: 0.05 °C/m); and Case 12 (G: 0.1 °C/m).

3.3. EWT and HER According to Operation Method

Figure 11 indicates the HER and the outlet temperature of the heat source water according to the operating methods. Under the flow rate of the heat source water conditions, the HER of Case 13 (*v*: 0.3504 m/s) showed a 2.26 W/m reduction compared to Case 1 (*v*: 0.292 m/s), but a 10% increase compared to Case 2 (*v*: 0.292 m/s), which is with a 300 m deep GHX. In addition, the HER of Case 16 (Limit Temperature: 0 °C), of which limit temperature was changed, showed a 19% and 37% gap with Case 1 (Limit Temperature: 5 °C) and Case 2 (*v*: 0.292 m/s), respectively. In this regard, it can be confirmed that the limit temperature condition can further improve the performance of the system.
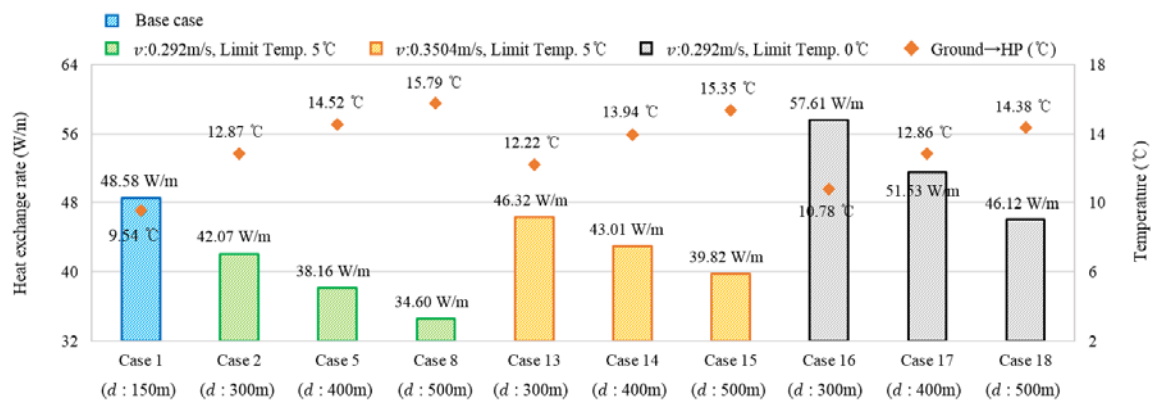
Figure 11. EWT and HER according to the operation method and the length of the GHX.

Figure 12 describes the total HER per borehole according to the operation method. As for the deep GHX, the HER in the case with a 500 m long heat exchanger results in up to 37% increase compared with the case with 300 m and 400 m long heat exchanger, and under the same condition of the length of the GHX, the operation method utilizing the limit temperature augmented the HER per borehole at the most. According to the flow rate changes, Case 18 (*v*: 0.292 m/s) showed a 16% higher HER per borehole, as much as 3.15 kW, compared to Case 15 (*v*: 0.3504 m/s) of which flow rate was increased, and was 33% higher, as much as 5.76 kW, than Case 8 without operation method.
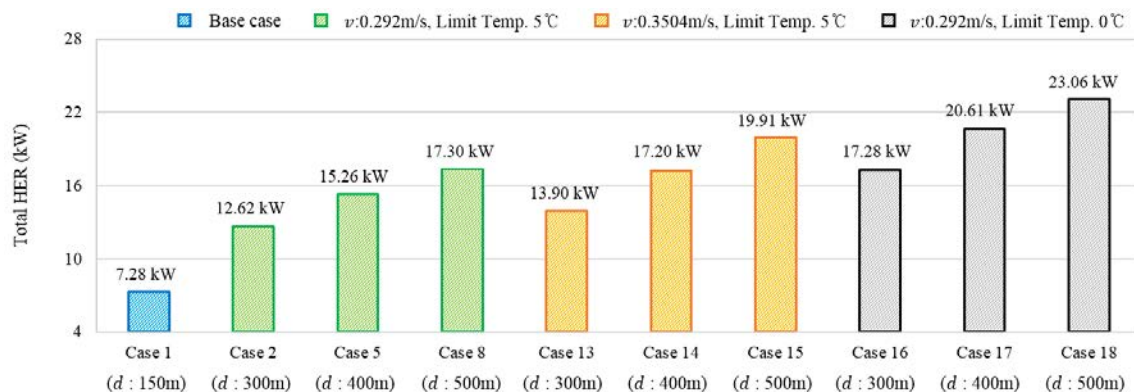
Figure 12. Total HER per borehole according to the operation method and the length of the GHX.

Based on a 500 m deep heat exchanger, the HER increased a maximum of around 15% in the case with flow rate changes and 33% in the case with the limit temperature. In this respect, it was confirmed that the limit temperature condition had more effect on the improvement of the system performance than the flow rate condition of the heat source water.

4. Feasibility Analysis of an Introduction of GSHP System Using Deep GHX

4.1. Overview of Feasibility Analysis

To conduct the feasibility analysis of introducing a geothermal heat pump system, a quantitative analysis on the amount of energy consumption of object building is needed. Thus, in this study, the "Design Standards for Office Building", presented by the "Korea Energy Economics Institute (KEEI)", was considered (Figure 13) [23,24].
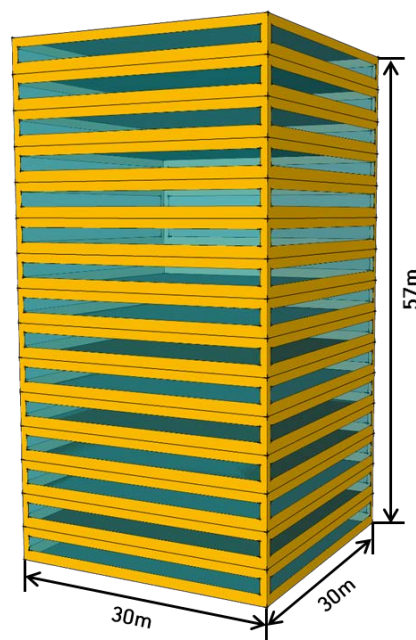
Figure 13. Model of office building.

TRNSYS 17 (University of Wisconsin-Madison, Madison, WI, USA), enabled to analyze the "Dynamic Thermal Loading", was used for the modeling of thermal loading. Annual heating and peak load were analyzed. Standard specifications set for the design of office building are summarized in Table 3.

Table 3. Standard specifications set for the design of office building.

Variables	Condition
Location	Seoul
Typical floor area	30 m × 30 m (900 m^2)
Number of floor	15 floor
Floor height	3.8 m
Window area ratio	40%

Table 4 shows conditions set for the simulation analysis of thermal loading. The climatic data of the region of Seoul Metropolis were used. The area of air conditioning was set as 80% of entire floor area of the building. The times required for the operation of heating system was set 9 h from 09:00 a.m. to 18:00 p.m. by taking the activities of occupants in the building into account. To set conditions of thermal insulation and set temperature for indoor heating of the building, the "Energy Saving Standards for the Design of Buildings", presented by Ministry of Land, Infrastructure and Transport, were referred to [25,26].

Table 4. Simulation conditions.

Variables	Condition
Weather data	Seoul
Facility area	720 m^2
Operation time	09:00–18:00 (9 h)
Operation period	1–3, 11–12 (5 months)
Heating set temperature	22 °C

4.2. Results of Simulation Analysis

Figure 14 shows the heating load varied during the period of operation of the model of thermal loading. The total heating load of entire period of analysis was 339.4 MW. Table 5 shows the peak load of each floor of object building. The peak heating load was 124.6 kW. The sum of peak loads at each floor of the object building was 1837.3 kW.
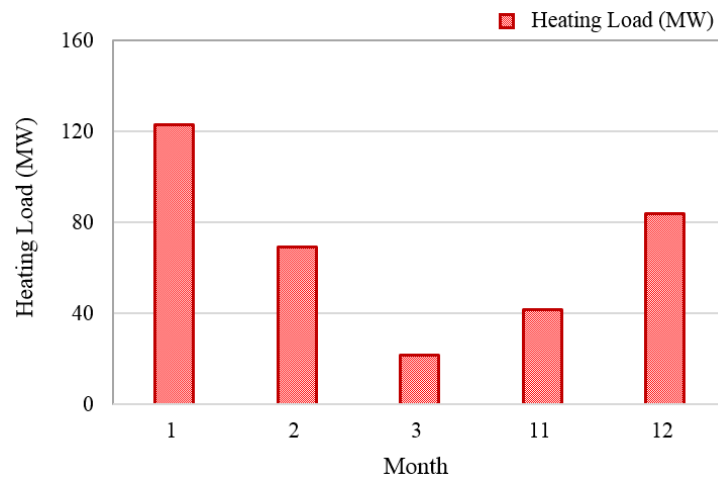

Figure 14. Monthly heating load of object building.

Table 5. Calculations of peak loads of each floor of object building.

	1F	2F	3F	4F	5F	6F	7F	8F
Peak load (kW)	115.1	123.6	123.9	123.7	123.5	123.3	123.3	123.3
	9F	10F	11F	12F	13F	14F	15F	Total
Peak load (kW)	123.3	123.4	123.6	123.6	123.8	123.4	115.2	1837.3

4.3. Calculation of Initial Investment

With the sum of peak loads at each floor, the system installation capacities for respective cases were calculated; the initial investment was then calculated based on the system installation capacities. For the calculation of drilling cost of the borehole occupying the highest weight among initial investment, an additional cost corresponding to the depth of borehole was considered. The rate of additional cost was set to be 10% of basic drilling cost from the point of depth of 100 m from ground surface of the borehole. Table 6 shows the unit drilling cost per meter at each interval of the depth of borehole.

Table 6. Unit Drilling Cost per Meter.

Drilling Depth (m)	Drilling Cost Per Meter (USD)
0–100	18
100–200	20
200–300	22
300–400	24
400–500	27

Table 7 represents the number of drilled boreholes and drilled depth of each case. Numbers of boreholes were calculated through the heat amount produced from each borehole corresponding to the sum of peak loads at each floor of the object building.

Table 7. Number of drilled boreholes and drilled depth of each case.

	Total HER (kW)	Number of Borehole	Total Drilling Depth (m)
Case 1	7.3	253	37,950
Case 2	12.6	146	43,800
Case 3	12.2	151	45,300
Case 4	11.7	157	47,100
Case 5	15.3	121	48,400
Case 6	14.9	124	49,600
Case 7	14.4	128	51,200
Case 8	17.3	107	53,500
Case 9	16.9	109	54,500
Case 10	16.5	112	56,000
Case 11	24.4	76	38,000
Case 12	31.9	58	29,000
Case 13	13.9	133	39,900
Case 14	17.2	107	42,800
Case 15	19.9	93	46,500
Case 16	17.3	107	32,100
Case 17	20.6	90	36,000
Case 18	23.1	80	40,000

Table 8 represents the initial investment for each case. Initial investment was calculated by adding labor cost to the material cost corresponding to each number of drilled boreholes presented in Table 7.

Table 8. Initial investment for each case (Unit: USD).

	Drilling	Casing	GHX	Grout	Superplasticizer	Circulating Pump	Heat Pump	Total
Case 1	816,500	333,684	255,300	177,675	18,630	36,800	94,091	1,732,680
Case 2	998,109	192,561	294,655	205,064	21,502	21,236	85,909	1,819,035
Case 3	1,032,291	199,155	304,745	212,086	22,238	21,964	85,909	1,878,389
Case 4	1,073,309	207,069	316,855	220,514	23,122	22,836	85,909	1,922,341
Case 5	1,153,020	159,588	325,600	226,600	23,760	17,600	81,818	1,987,986
Case 6	1,181,607	163,545	333,673	232,218	24,349	18,036	81,818	2,035,246
Case 7	1,219,724	168,820	344,436	239,709	25,135	18,618	81,818	2,098,260
Case 8	1,333,628	141,124	359,909	250,477	26,264	15,564	77,727	2,204,693
Case 9	1,358,556	143,761	366,636	255,159	26,755	15,855	77,727	2,244,449
Case 10	1,395,947	147,718	376,727	262,182	27,491	16,291	77,727	2,304,084
Case 11	947,250	100,237	255,636	177,909	18,655	11,055	69,545	1,580,287
Case 12	722,902	76,496	195,091	135,773	14,236	8,436	61,364	1,214,298
Case 13	91,055	175,415	268,418	186,805	19,587	19,345	85,909	1,755,625
Case 14	1,019,613	141,124	287,927	200,382	21,011	15,564	81,818	1,812,893
Case 15	1,159,135	122,658	312,818	217,705	22,827	13,527	77,727	1,926,398
Case 16	731,491	141,124	215,945	150,286	15,758	15,564	85,909	1,356,077
Case 17	857,618	118,702	242,182	168,545	17,673	13,091	85,909	1,503,720
Case 18	997,105	105,513	269,091	187,273	19,636	11,636	81,818	1,672,073

4.4. Calculation of Annual Operation Cost

In the present study, the HER of geothermal heat pump system, the outlet temperature of circulation pump, and the entering water temperature (EWT) were predicted. The coefficient of heating performance (H.COP) of geothermal heat pump was calculated by referring to the performance curve of geothermal heat pump calculated in the previous study (Figure 15).
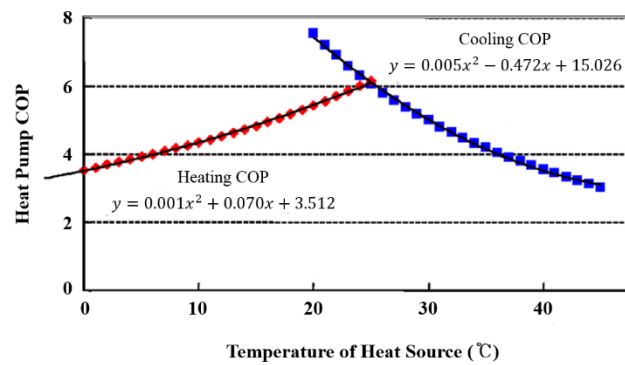
Figure 15. Heat pump COP [27].

Table 9 shows the amount of monthly power consumption and coefficient of heating performance of geothermal heat pump for each case. The power consumption of geothermal heat pump was calculated using the coefficient of heating performance of geothermal heat pump. The amount of power consumption of circulation pump was assumed to be 250 W per borehole. The total amount of monthly power consumption is the sum of monthly power consumptions of the geothermal heat pump and circulation pump.

Table 9. EWT, H.COP and monthly power consumption of each case.

	EWT (°C)	H.COP	Jan. Power Consumption (MWh)	Feb. Power Consumption (MWh)	Mar. Power Consumption (MWh)	Nov. Power Consumption (MWh)	Dec. Power Consumption (MWh)
Case 1	9.54	4.27	28.78	16.25	5.05	9.79	19.59
Case 2	12.87	4.58	26.84	15.16	4.72	9.13	18.27
Case 3	12.61	4.55	26.99	15.24	4.74	9.18	18.37
Case 4	12.30	4.52	27.16	15.34	4.77	9.24	18.49
Case 5	14.52	4.74	25.93	14.64	4.56	8.82	17.65
Case 6	14.27	4.71	26.07	14.72	4.58	8.87	17.75
Case 7	13.96	4.68	26.24	14.81	4.61	8.93	17.86
Case 8	15.79	4.87	25.25	14.26	4.44	8.59	17.19
Case 9	15.56	4.84	25.37	14.33	4.46	8.63	17.27
Case 10	15.27	4.81	25.53	14.41	4.48	8.69	17.38
Case 11	20.21	5.34	23.04	13.01	4.05	7.84	15.68
Case 12	28.64	6.34	19.39	10.95	3.41	6.60	13.20
Case 13	12.22	4.52	27.21	15.36	4.78	9.26	18.52
Case 14	13.94	4.68	26.25	14.82	4.61	8.93	17.87
Case 15	15.35	4.82	25.49	14.39	4.48	8.67	17.35
Case 16	10.78	4.38	28.04	15.83	4.93	9.54	19.09
Case 17	12.86	4.58	26.85	15.16	4.72	9.14	18.28
Case 18	14.38	4.73	26.01	14.68	4.57	8.85	17.71

Table 10 presents the cost for the operation of heating system. To calculate the cost of power consumption for the operation of heating system, the "General Electric Rates Standards" presented by Korea Electric Power Corporation (KEPCO) were referred to [28]. Overall cost of the operation of heating system was comprised of the costs of power consumption required for the operation of heat pump and circulation pump.

Table 10. Total operation cost of heating system for each case (Unit: USD).

	Heat Pump Electric Charge	Circulating Pump Electric Charge	System Electric Charge	VAT	Total Cost
Case 1	68,466	9185	77,652	7765	85,416
Case 2	67,648	5300	72,949	7295	80,244
Case 3	67,710	5482	73,193	7319	80,512
Case 4	67,785	5700	73,485	7348	80,833
Case 5	67,264	4393	71,656	7165	78,822
Case 6	67,321	4502	71,823	7182	79,005
Case 7	67,393	4647	72,040	7204	79,244
Case 8	66,976	3885	70,861	7086	77,947
Case 9	67,028	3957	70,985	7098	78,084
Case 10	67,093	4066	71,159	7115	78,275
Case 11	66,038	2759	68,797	6880	75,677
Case 12	64,498	2105	66,604	6660	73,264
Case 13	67,804	4828	72,633	7264	79,895
Case 14	67,397	3885	71,282	7128	78,410
Case 15	67,075	3376	70,451	7045	77,496
Case 16	68,155	3885	72,040	7204	79,244
Case 17	67,651	3267	70,918	7092	78,010
Case 18	67,295	2905	70,200	7020	77,220

4.5. Results of Economy Analysis

For the analysis of the economy of heating system, the installations of existing system and the system developed in the present study in the model of heat load analysis were assumed. By calculating the initial investment and annual operation cost for each case, the life cycle cost (LCC) and return on investment (ROI) for each case were analyzed. In the present study, the net present value (NPV), as expressed in the following equations, was used for the analysis.

$$P = P_F + P_A \tag{10}$$

$$P_F = \frac{C_F}{(1 + I_r)^n} \tag{11}$$

$$P_A = \frac{C_A[(1 + I_r) - 1]}{(1 + I_r)^n} \tag{12}$$

$$I_r = \frac{(1 + I_n)}{(1 + F)} - 1 \tag{13}$$

The average value of 3.61%, set for the national bond of five years maturity during 10 years (2007–2016) presented in the Korea Bank Economic Statics System notified by the Bank of Korea was taken as nominal discount rate. The period of 30 years was used for the analysis. The cases of initial investment, recovered by the sum of return on investment in 10 years, were concluded as economically feasible ones. The times to maintenance of the heat and circulation pumps were set as five years and three years, respectively, while the times to replacement of each pump were set as ten years and six years, respectively.

Figure 16 shows the results of LCC analysis for each case. With the depth of 300 m of the GHX, the corresponding initial investment exceeded by 5% the initial investment of existing system (150 m) while the annual operation cost thereof appeared lower than that of existing system by 6.5%; this resulted in 12 years of complete recovery of initial investment. However, in cases where the depth of GHX exceeded 400 m in the same ground, the initial investment was not recovered during the period.
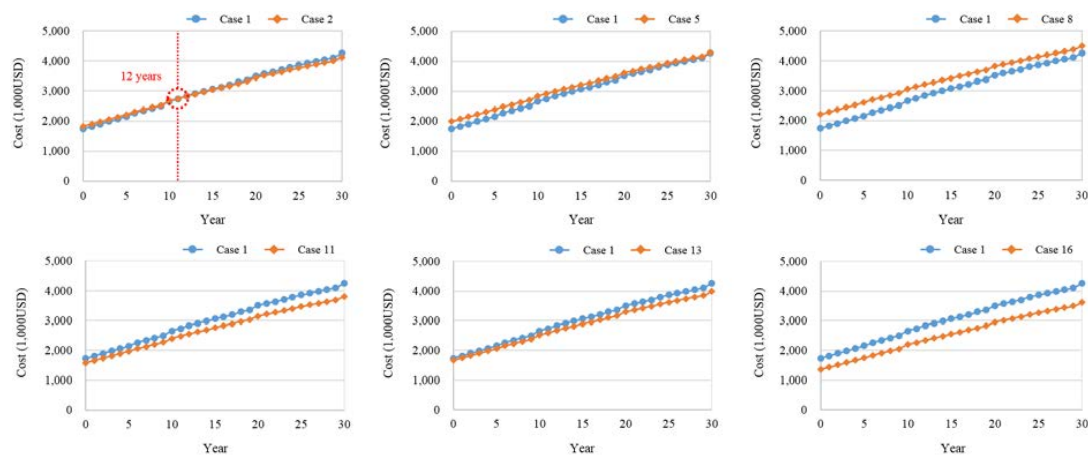
Figure 16. Comparison of LCC and Periods of the Recovery of Initial Investment.

The operation of heating system with the flow rate of circulation water increased by over 20% in the same ground condition resulted in over 91% more heat being collected than the existing system, which enabled the securing of economic feasibility through reduced length of the borehole. In addition, even under the condition of the limit temperature of circulation water reduced to 0 °C, the collected heat amount reached the level more than 2.4 times that of existing system, which also enabled the economic feasibility of the heating system through the introduction of operational schemes. Besides, under conditions of the geothermal gradient of over 0.05 °C/m (Cases 11 and 12), the collection of high temperature geo-heat was available with reduced entire length of the installation of the GHX, which was found more economical than the existing system.

5. Conclusions

In this study, a method to develop a geothermal heat pump system using a deep GHX was proposed, and a numerical simulation was utilized by establishing a geothermal and groundwater transfer model coupled with a deep GHX model. With the simulation results, the HER was quantitatively analyzed using the underground condition and control method of the geothermal heat pump system. The results of this study are summarized as follows.

1. According to the HER per unit meter, Case 1 (*GHX*: 150 m), which is a general geothermal system, has a 15% higher amount than that of Case 2 (*GHX*: 300 m), which is a geothermal system with a deep heat exchanger. As for the HER per unit borehole, however, Case 2 showed about 73% higher performance than Case 1. As a result, it was confirmed that the performance of heat exchange was improved by supplying the heat source with high temperature based on the geothermal gradient as the length of the ground heat exchange increased.

2. As the length of the GHX became longer, the HER per unit meter decreased, but the total amount per unit borehole increased. The HER per unit meter in Case 8 (*GHX*: 500 m) was 22% lower than that of Case 2 (*GHX*: 300 m); however, the total amount of borehole was increased by 37%, which was 4.68 kW higher. In addition, the outlet temperature of the heat source water increased 2.92 °C from Case 2 (*GHX*: 300 m) to Case 8 (*GHX*: 500 m), and the slope of the heat exchange value during the operation period was gentle. Therefore, it was found that the potential to further extract the underground heat source could improve as the length increases.

3. Under the same condition of a 500 m long heat exchanger, the analysis results comparing Case 8 (*G*: 0.02 °C/m) with Case 12 (*G*: 0.1 °C/m) showed that the HER of Case 12 increased about 84% compared Case 8, and the outlet temperature difference of the heat source water was 12.85 °C. Additionally, the potential of the system was enhanced as the geothermal gradient increases, so that it can be expected that operation methods and design conditions are required to maximize the potential of the system when installing a deep GHX in a geothermal gradient region.

4. Regarding the flow rate of the heat source water, the HER of Case 15, of which flow rate was set as 0.3504 m/s, showed 5.22 W/m higher than that of Case 8 (*v*: 0.292 m/s) which has lower flow rate. In addition, the HER in the condition of 500 m length of heat exchanger was about 15% different from that of 300 m length and 400 m length.

5. When the length of the heat exchanger is 300 m, the HER according to the limit temperature was 15.54 W/m in Case 16 (Limit Temperature: 0 °C), which is higher than that of Case 2 (Limit Temperature: 5 °C), and this performance showed up to 37% difference according to the limit temperature.

6. Comparing the HER per unit borehole of Case 8 (*v*: 0.292 m/s) with those of Case 15 (*v*: 0.3504 m/s) and Case 18 (Limit Temperature: 0 °C), those of Cases 15 and 18 were increased by a maximum of 15% and 33%, respectively. In this regard, it was confirmed that the operation method using the limit temperature has more influence on the improvement of the system performance.

7. The initial investment payback period of Case 2 (*GHX*: 300 m) of GSHP system using deep GHX compared to general GSHP system Case 1 (*GHX*: 150 m) was confirmed to be 12 years. However, as the depth of GHX increases, the installation cost increased and it was difficult to secure cost savings.

8. In Case 12 (*G*: 0.1 °C/m) with high geothermal gradient, the GSHP system using deep GHX saved initial investment cost up to 518,382 USD compared to general GSHP system. It is more economical than general GSHP system in high temperature gradient conditions.

In the future, experimental approach of GSHP with a deep well will be conducted through the real application. Furthermore, a boring technic for deep GHX will be developed considering suitable diameter and depth.

Author Contributions: The authors Sang Mu Bae and Yujin Nam defined the performance analysis models, developed the methodology and wrote the full manuscript. The author Byoung Ohan Shim checked the results and the whole manuscript.

Conflicts of Interest: The authors declare no conflict of interest.

References

1. Majuri, P. Technologies and environmental impacts of ground heat exchangers in Finland. *Geothermics* **2014**, *73*, 124–132. [CrossRef]
2. Cho, S.; Ray, S.; Im, P.; Honari, H.; Ahn, J. Methodology for energy strategy to prescreen the feasibility of Ground Source Heat pump systems in residential and commercial buildings in the United States. *Energy Strategy Rev.* **2017**, *18*, 53–62. [CrossRef]
3. Li, C.; Cleall, P.J.; Mao, J.; Muñoz-Criollo, J.J. Numerical simulation of ground source heat pump systems considering unsaturated soil properties and groundwater flow. *Appl. Therm. Eng.* **2018**, *139*, 307–316. [CrossRef]
4. Park, J.-I.; Park, K.S. Analysis of earth design parameter and geothermal heat exchanger length in geothermal system. *Trans. Korea Soc. Geotherm. Energy Eng.* **2015**, *11*, 1–6. [CrossRef]
5. Hahn, J.-S.; Han, H.-S.; Hahn, C. *Geothermal Energy*; Hanrimwon: Seoul, South Korea, 2010.
6. Huchtemann, K.; Müller, D. Combined simulation of a deep ground source heat exchanger and an office building. *Build. Environ.* **2014**, *73*, 97–105. [CrossRef]
7. Holmberg, H.; Acuña, J.; Næss, E.; Sønju, O.K. Thermal evaluation of coaxial deep borehole heat exchangers. *Renew. Energy* **2016**, *97*, 65–76. [CrossRef]
8. Le Lous, M.; Larroque, F.; Dupuy, A.; Moignard, A. Thermal performance of a deep borehole heat exchanger: Insights from a synthetic coupled heat and flow model. *Geothermics* **2015**, *57*, 157–172. [CrossRef]

9. Michopoulos, A.; Kyriakis, N. Predicting the fluid temperature at the exit of the vertical ground heat exchangers. *Appl. Energy* **2009**, *86*, 2065–2070. [CrossRef]

10. Chen, S.; Mao, J.; Han, X. Heat transfer analysis of a vertical ground heat exchanger using numerical simulation and multiple regression model. *Energy Build.* **2016**, *129*, 81–91. [CrossRef]

11. Li, W.; Wang, Y.; Jin, Y. Study on Heat Transfer Calculation Method of Ground Heat Exchangers Based on Heat Pump Unit Operation Characteristics. *Procedia Eng.* **2016**, *146*, 450–458. [CrossRef]

12. Park, J.I.; Park, K.S. Study on Capacity Alteration of Geothermal Heat Exchanger by Changing Design Condition. *Trans. Korea Soc. Geotherm. Energy Eng.* **2013**, *9*, 8–13. [CrossRef]

13. Kim, E.J. Impact of Different Boundary Conditions in Generating g-function on the Sizing of Ground heat Exchangers. *Korean J. Air Cond. Refrig. Eng.* **2014**, *26*, 263–268. [CrossRef]

14. Shin, Y.H.; Tansehen, M.R.; Chung, H.C.; Jeong, H.M. A study on the Yearly Measurement and Numerical Analysis of Underground Temperature. *J. Korean Soc. Power Syst. Eng.* **2012**, *16*, 30–35. [CrossRef]

15. Min, K.C.; Choi, J.H. Effect of the Design Parameters of Geothermal Heat Exchanger Design Length. *Trans. Korea Soc. Geotherm. Energy Eng.* **2011**, *7*, 10–15.

16. Ryoo, Y.-S.; Kim, J.-H.; Jeong, S.-H. Performance Evaluation of Closed Coaxial Ground Heat Exchanger in the case of 2000 m-Depth Single Well. *J. Korean Soc. Manuf. Process Eng.* **2016**, *15*, 83–92.

17. Uchida, Y.; Sakura, Y.; Taniguchi, M. Taniguchi, Shallow subsurface thermal regimes in major plains in Japan with reference to recent surface warming. *Phys. Chem. Earth Parts A B C* **2003**, *28*, 457–466. [CrossRef]

18. Stutz, G.R.; Shope, E.; Aguirre, G.A.; Batir, J.; Frone, Z.; Williams, M.; Reber, T.J.; Whealton, C.A.; Smith, J.D.; Richars, M.C.; et al. Geothermal energy characterization in the Appalachian Basin of New York and Pennsylvania. *Geosphere* **2015**, *11*, 1291–1304. [CrossRef]

19. Kim, M.; Kim, H. Domestic geothermal energy distribution. *Korea J. Geotherm. Energy* **2005**, *1*, 33–38.

20. Fujii, H.; Itoi, R.; Fujii, J.; Uchida, Y. Optimizing the design of large-scale ground-coupled heat pump systems using groundwater and heat transport modeling. *Geothermics* **2005**, *34*, 347–364. [CrossRef]

21. Diersch, H.J.G. *FEFLOW Reference Manual*; WASY GmbH: Berlin, Germany, 2009.

22. Nam, Y.; Ooka, R.; Hwang, S. Development of a numerical model to predict heat exchange rates for a ground-source heat pump system. *Energy Build.* **2008**, *40*, 2133–2140. [CrossRef]

23. Choi, D.Y.; Choi, M.S.; Kim, J.I.; Park, T.S.; Lee, G.H.; Seo, D.H. *National Building Energy Consumption Permanent Sample Survey Research*; Korea Energy Economics Institute (KEEI): Ulsan, South Korea, 2015.

24. Lee, H.W. Performance-based Energy Standard of the Total Annual Energy Use in Office and Apartment Buildings. *J. Korea Soc. Living Environ. Syst.* **2008**, *15*, 596–602.

25. *Design Standard for Energy Conservation in Building, Asterisk 1—Percentage of Thermal Transmittance in Building Area by Region*; Ministry of Land, Infrastructure and Transport: Sejong-si, South Korea, 2017.

26. *Design Standard for Energy Conservation in Building, Asterisk 8—Indoor Temperature and Humidity Standard for Calculating the Capacity of the Heating and Cooling Equipment*; Ministry of Land, Infrastructure and Transport: Sejong-si, South Korea, 2017.

27. Nam, Y.J. Numerical Analysis for the Effect of Ground and Groundwater Conditions on the Performance of Ground Source Heat Pump System. *Korean J. Air Cond. Refrig. Eng.* **2011**, *23*, 321–326. [CrossRef]

28. Korea Electric Power Corporation (KEPCO). *General Service, Electric Rates Table*; Korea Electric Power Corporation (KEPCO): South Korea, 2017.